Available online at www.sciencedirect.com
ScienceDirect
Scripta Materialia 56 (2007) 69–72
Scripta MATERIALIA
www.actamat-journals.com

Effect of welding parameters on tensile properties and fracture behavior of friction stir welded Al–Mg–Si alloy

S.R. Ren, Z.Y. Ma* and L.Q. Chen

Institute of Metal Research, Chinese Academy of Sciences, 72 Wenhua Road, Shenyang 110016, China

Received 13 June 2006; revised 16 August 2006; accepted 21 August 2006
Available online 2 October 2006

Al–Mg–Si alloy plates friction stir welded at a tool traverse speed of 400 mm/min exhibited higher tensile strength with 45° shear fracture, whereas lower tensile strengths with nearly vertical fractures were observed for samples welded at a lower speed of 100 mm/min. The fracture paths corresponded well with the lowest hardness distribution profiles in the joints. The heat indexes cannot be used as parameters to evaluate the thermal input, mechanical properties and fracture mode.

Keywords: Friction stir welding; Aluminum alloy; Property; Fracture

Friction stir welding (FSW) is a relatively new solid-state joining technique and has been extensively developed for aluminum alloys, as well as for magnesium, copper, titanium and steel [1,2]. Compared to conventional fusion welding methods, the advantages of the FSW process include better mechanical properties, low residual stress and distortion, and reduced occurrence of defects [1,2].

For FSW, both tool rotation rate (ω) and traverse speed (v) exert a significant effect on the thermal input and mechanical properties. It was reported that the peak temperature in the FSW zone increases with increasing tool rotation rate in 6061Al–T6, 1050Al and 6063Al–T5 [3–5]. Furthermore, the peak temperature in the weld zone increases with increasing ω/v ratio in 2024Al–T6, 5083Al–O and 7075Al–T6 [6]. On the other hand, Lee et al. [7] reported that the hardness of the weld nugget of FSW 6061Al at higher rotation rates was higher than that at lower rotation rates due to a higher density of spherical-shaped reprecipitates. Furthermore, both strength and elongation of 6061Al–T651 decreased with decreasing traverse speed and increasing rotation rate [8]. However, when both rotation rate and traverse speed change, it is hard to evaluate quantitatively the parameter dependence of the thermal input and mechanical properties. Based on experimental observations, Arbegast and Hartley [9] suggested a unitized parameter – the pseudo heat index ω^2/v – to describe the parameter dependence of the thermal input. It was shown that for several aluminum alloys, a general relationship between maximum temperature and FSW parameters can be expressed by

$$\frac{T}{T_m} = K\left(\frac{\omega^2}{v \times 10^4}\right)^{\alpha} \tag{1}$$

where the exponent α was reported to range from 0.04 to 0.06, the constant K is between 0.65 and 0.75, and T_m (°C) is the melting point of the alloy.

For FSW aluminum alloys, three distinct zones – the stirred zone (SZ), the thermomechanically affected zone (TMAZ) and the heat-affected zone (HAZ) – are identified based on microstructural characterization of grains and precipitates [2]. The HAZ experiences a thermal cycle, but does not undergo any plastic deformation. Mahoney et al. [10] defined the HAZ as a zone experiencing a temperature rise above 250 °C for a heat-treatable aluminum alloy. The HAZ retains the same grain structure as the parent material. However, the thermal exposure above 250 °C results in significant coarsening of the precipitates and development of the precipitate-free zone (PFZ). Thus, the HAZ exhibits the lowest hardness and strength, and the fracture occurs usually in the HAZ [2,11,12]. Because the microstructure of the HAZ is mainly determined by the thermal input during the FSW, it is worthwhile to check if the pseudo heat index ω^2/v can be used to evaluate the parameter

* Corresponding author. Tel./fax: +86 24 83978908; e-mail: zyma@imr.ac.cn

1359-6462/$ - see front matter © 2006 Published by Elsevier Ltd. on behalf of Acta Materialia Inc.
doi:10.1016/j.scriptamat.2006.08.054

dependence of the mechanical properties and the fracture behavior of FSW aluminum alloys.

In this study, the hardness distribution, tensile properties and fracture characteristics of 6061Al–T651 plates, friction stir welded at the same heat indexes but different rotation rates and traverse speeds, were investigated to examine the effect of the welding parameters on the mechanical properties and the fracture behavior of FSW aluminum alloys.

The material used was 6 mm thick 6061Al–T651 rolled plate. The chemical composition and tensile properties of the plate are shown in Table 1. The samples were longitudinally butt-welded using a FSW machine (China FSW Center). A tool with a shoulder of 24 mm in diameter and a threaded cylindrical pin of 6 mm in diameter was used. The welding parameters used in this study are summarized in Table 2. The same pseudo heat indexes, ω^2/v, of 1600 and 3600 were used for samples 1 and 3 and for samples 2 and 4, respectively. On the other hand, samples 1 and 5 have the same ω/v ratio. After welding, the joints were cross-sectioned perpendicular to the welding direction for optical examination, hardness measurement and tensile test. The configuration and size of the transverse tensile specimens are shown in Figure 1. Vickers microhardness distribution maps were measured at an interval of 1 mm in the regions 8–19 mm from the weld center on both retreating and advancing sides. Hardness measurement was conducted on an automatic testing machine (Leco, LM-247AT) under a load of 300 g for 15 s. Room-temperature tensile tests were carried out at a strain rate of 4×10^{-4} s^{-1} on a universal testing machine (AG-5000A). The property data for each weld were obtained by averaging two test results.

Figure 2 shows the cross-sectional macrostructures of FSW 6061Al–T651. Under investigated welding parameters, no welding defect was detected in the joints. Three microstructural zones – SZ, TMAZ and HAZ – were discernible. The shapes of the weld zone were apparently parameter dependent. For the same ω^2/v or ω/v, the SZ had quite different shapes. Generally, the SZ consisted of upper and lower parts, and no complete and uniform nugget morphology was observed. A similar phenomenon was found in FSW 6061Al [13], but not in other FSW aluminum alloys [2]. There were saw teeth in the SZ of samples 1 and 4. A similar phenomenon has been

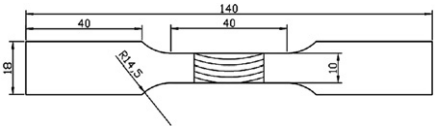

Figure 1. Configuration and size of tensile specimens.

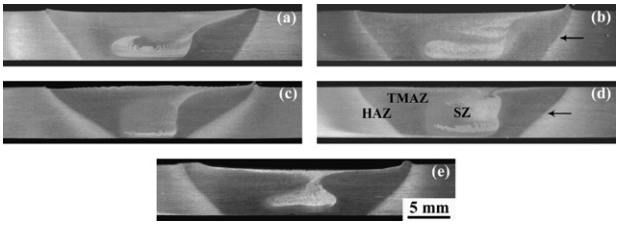

Figure 2. Cross-sectional macrostructures of FSW 6061Al–T651: (a) 400 rpm, 100 mm/min; (b) 600 rpm, 100 mm/min; (c) 800 rpm, 400 mm/min; (d) 1200 rpm, 400 mm/min and (e) 1600 rpm, 400 mm/min. The advancing side of the weld is on the right in all the macrographs.

observed in FSW 6061Al joint by Liu et al. [13]. Furthermore, it is noted that there are distinct boundaries (as shown by arrows in Fig. 2) in the HAZ that separated two parts with different etching contrasts. For the lower traverse speed of 100 mm/min, the boundaries exhibited an inclination of ~30° to the butting surface, whereas at the higher traverse speed of 400 mm/min, the inclination of the boundaries increased to ~45°. The tool rotation rate did not exert a significant effect on the inclination of these boundaries.

The hardness profile of the FSW joints is a direct indicator of microstructural evolution during FSW. The fracture of FSW heat-treatable aluminum alloys usually occurs in the HAZ, i.e. the softest zone in the FSW joints, due to significant coarsening of the precipitates [2,10,13,14]. In previous studies, the hardness profile was measured either along the mid-thickness of the FSW plate or along the top, center and bottom of the plate thickness to determine the lowest hardness point [2]. In this case, however, the lowest hardness profile throughout the plate thickness that might govern directly the fracture mode could not be established. In this

Table 1. Chemical compositions and mechanical properties of 6061Al–T651 plate

Chemical composition (wt.%)						Mechanical properties		
Mg	Si	Fe	Cu	Zn	Mn	UTS (MPa)	YS (MPa)	El. (%)
0.6–1.2	0.4–0.8	0.7	0.15–0.40	0.25	0.15	308	285	18

Table 2. Welding parameters and transverse tensile properties of FSW 6061Al–T651 joints

Sample no.	Rotation rate (ω) (rpm)	Welding speed (v) (mm/min)	ω^2/v	ω/v (r/mm)	YS (MPa)	UTS (MPa)	El. (%)	UTS_{FSW}/UTS_{base}
1	400	100	1600	4	117	188	11.8	0.61
2	600	100	3600	6	114	186	11.7	0.60
3	800	400	1600	2	141	215	8.5	0.70
4	1200	400	3600	3	138	217	11.4	0.70
5	1600	400	6400	4	136	206	10.7	0.67

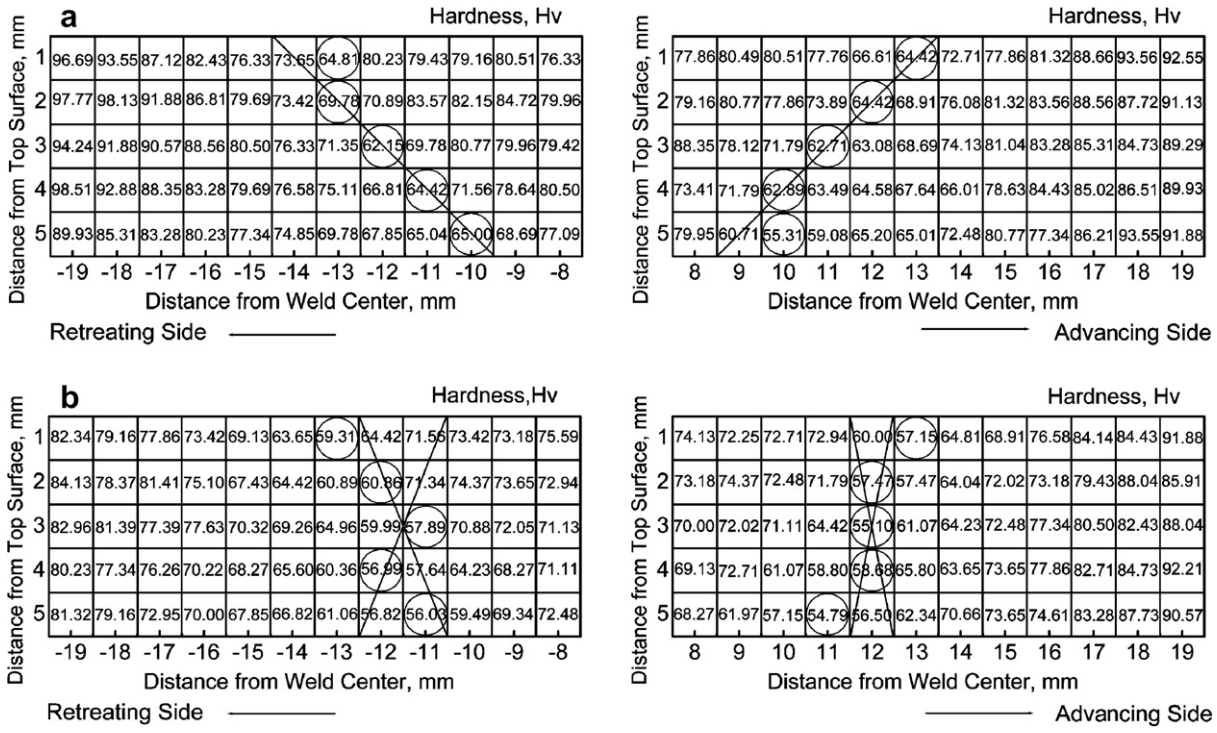

Figure 3. Microhardness maps of FSW 6061Al–T651: (a) 1200 rpm, 400 mm/min and (b) 600 rpm, 100 mm/min.

study, the hardness distribution map of the FSW samples was measured throughout the plate thickness. Figure 3 shows two typical hardness maps of the FSW joints at the same ω^2/v of 3600 (samples 2 and 4). Three important observations can be made. First, generally, the FSW joint welded at the higher traverse speed of 400 mm/min exhibited higher hardness values than that at the lower traverse speed of 100 mm/min, indicating that the thermal exposure experienced by the former was less than that experienced by the latter. Second, the lowest hardness distribution profiles of the weld at 400 mm/min exhibit a ~45° angle to the butting surface on both advancing and retreating sides, whereas the lowest hardness profiles of the weld at 100 mm/min were nearly parallel to the butting surface, especially on the advancing side. The lowest hardness profiles correspond well to the boundaries as shown by arrows in Figure 2 in both inclination and location. Third, the lowest hardness values on the advancing side were generally lower than those on the retreating side. This is attributed to a higher temperature on the advancing side where the tangential velocity vector direction was the same as that of the forward velocity vector [9].

The transverse tensile properties of FSW 6061Al–T651 joints are summarized in Table 2, which reveals the following important findings. First, compared to the base metal, the FSW joints exhibited reduced strength and ductility due to the overaged microstructure and localized deformation in the HAZ [10]. Second, for the same tool traverse speed, the rotation rate exerted no noticeable effect on the tensile properties of the FSW joints except for sample 3, which exhibited a reduced ductility. Third, irrespective of the tool rotation rate, the increase in the traverse speed from 100 to 400 mm/min increases significantly the yield and tensile strengths of the FSW joints, i.e. the strength of the FSW joints is mainly controlled by the tool traverse speed under the welding parameters investigated here. For the higher tool traverse speed of 400 mm/min, the FSW joints exhibited a joint efficiency (UTS_{FSW}/UTS_{base}) of 67–70%, which is in good agreement with that (67–79%) in FSW 6061Al reported by other investigators [15,16], whereas at the lower traverse speed of 100 mm/min, a lower joint efficiency of 60–61% was observed. Such a variation trend in strength is consistent with the hardness distribution maps of the FSW joints in which the hardness values of the weld at 400 mm/min were higher than those at 100 mm/min (Fig. 3). Fourth, the FSW joints, prepared at the same heat index, ω^2/v or ω/v, did not exhibit the same tensile properties, indicating that both heat indexes cannot be used as the parameters to describe the tensile properties of the welds.

Figure 4 shows the failed tensile specimens. Four important observations can be made. First, most of the FSW joints failed on the advancing side except for sample 3, which failed on the retreating side. This is consistent with other reports on FSW aluminum alloys [2,10]. Second, the tool traverse speed exerted a

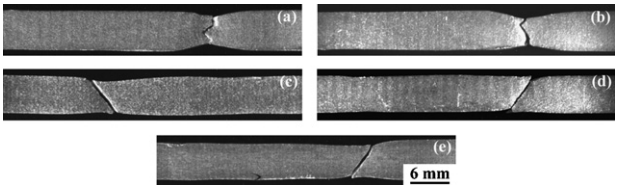

Figure 4. Appearance of failed FSW 6061Al–T651 joints: (a) 400 rpm, 100 mm/min; (b) 600 rpm, 100 mm/min; (c) 800 rpm, 400 mm/min; (d) 1200 rpm, 400 mm/min and (e) 1600 rpm, 400 mm/min. The advancing side of the weld is on the right in all the macrographs.

significant effect on the fracture mode of the FSW joints. At the higher traverse speed of 400 mm/min, failure occurred as shear fracture with limited necking (Fig. 4(c)–(e)). This observation is in good agreement with that by Mahoney et al. [10] on FSW 7075Al–T651. The shear fracture path was a 45° angle to the tensile axis, which corresponds well with the lowest hardness distribution profile (Fig. 3(a)). However, at the lower traverse speed of 100 mm/min, failure occurred nearly vertical to the tensile axis with distinct local necking and reduction in area (Fig. 4(a) and (b)). The fracture path corresponds with the lowest hardness distribution profile (Fig. 3(b)). Clearly, the fracture mode of the FSW joints was controlled by the lowest hardness distribution profiles, i.e. by the traverse speed under the welding parameters investigated here. Third, for the same tool traverse speed, the variation in the rotation rate did not change the fracture mode. For example, at 400 mm/min, the welds exhibited the same shear fracture mode under rotation rates of 800–1600 rpm. Fourth, the FSW joints, welded at the same heat index, ω^2/v or ω/v, did not exhibit the same fracture mode, indicating that these two heat indexes are not valid parameters to evaluate the fracture behavior of the welds.

The hardness profiles of the FSW joints, especially in the HAZ, are mainly governed by thermal exposure during FSW. Arbegast and Hartley [9] reported that the maximum temperature during the FSW thermal cycle can be expressed by Eq. (1), i.e. by a function of the pseudo heat index, ω^2/v. In this study, the same two pseudo heat indexes of 1600 and 3600 were used for samples 1–4. The different hardness profiles, shown in Figure 3, indicate that the thermal input during the FSW cannot be rationalized by a simple unitized parameter, ω^2/v. Furthermore, for the same ω^2/v, FSW 6061Al–T651 joints exhibited quite different tensile properties and fracture behaviors (Table 2 and Fig. 4). Therefore, the pseudo heat index, ω^2/v, cannot be used to evaluate the mechanical properties and fracture behavior of FSW aluminum joints. Similarly, another heat index, ω/v, was also proved to be invalid in predicting the tensile properties and fracture mode of the FSW joints.

The overaging of the HAZ is determined by both temperature and duration of thermal exposure during FSW, which are controlled by two competitive processes – heat generation and heat dissipation. The heat generation is mainly determined by the tool rotation rate. Increasing the rotation rate results in increased friction heat due to the increase in the tangential velocity of the tool. The heat dissipation is mainly controlled by the tool traverse speed. Increasing the traverse speed increases heat dissipation rate because the heated FSW zone is quickly brought into cool base metal, resulting in reduced temperature and duration of thermal exposure in the HAZ. It is very likely that the heat dissipation is a dominant factor affecting the thermal exposure under the welding parameters investigated in this study. In this case, the tool traverse speed becomes the dominant factor in determining the thermal exposure, mechanical properties and fracture behavior of FSW 6061Al–T651 joints. The increase in the tool traverse speed results in reduced thermal exposure, thereby increasing the hardness and strength of the welds.

In summary, the following conclusions are reached:

1. For FSW 6061Al–T651, the lowest hardness distribution profiles were a 45° angle with the butting surface of the joints welded at the higher traverse speed of 400 rpm, whereas the lowest hardness profiles nearly vertical to the butting surface were observed at the lower traverse speed of 100 mm/min.
2. FSW 6061Al–T651 joints welded at 400 mm/min exhibited higher strength with a 45° shear fracture, whereas a lower tensile strength with nearly vertical fractures were observed for the samples welded at 100 mm/min. The fracture paths corresponded well with the lowest hardness distribution profiles.
3. Both heat indexes, ω^2/v and ω/v, cannot be used as the parameters to describe the thermal input, tensile properties and fracture behavior of FSW 6061Al–T651. Under the welding parameters investigated in this study, the traverse speed appears to be a dominant factor in determining the tensile properties and fracture mode of the welds.

This work was supported by the Hundred Talents Project of Chinese Academy of Sciences and by the National Outstanding Young Scientist Foundation (under Grant No. 50525103).

[1] W.M. Thomas, E.D. Nicholas, J.C. Needham, M.G. Murch, P. Templesmith, C.J. Dawes, GB Patent Application No. 9125978.8, December 1991.
[2] R.S. Mishra, Z.Y. Ma, Mater. Sci. Eng. R 50 (2005) 1.
[3] W. Tang, X. Guo, J.C. McClure, L.E. Murr, J. Mater. Process. Manu. Sci. 7 (1998) 163.
[4] Y.J. Kwon, N. Saito, I. Shigematsu, J. Mater. Sci. Lett. 21 (2002) 1473.
[5] Y.S. Sato, M. Urata, H. Kokawa, Metall. Mater. Trans. A 33 (2002) 625.
[6] T. Hashimoto, S. Jyogan, K. Nakata, Y.G. Kim, M. Ushio, in: Proceedings of the First International Symposium on Friction Stir Welding, Thousand Oaks, CA, June 14–16, 1999.
[7] W.B. Lee, Y.M. Yeon, S.B. Jung, Mater. Trans. 45 (2004) 1700.
[8] S. Lim, S. Kim, C. Lee, C.G. Lee, S. Kim, Metall. Mater. Trans. A 35 (2004) 2829.
[9] W.J. Arbegast, P.J. Hartley, in: Proceedings of the Fifth International Conference of Trends in Welding Research, Pine Mountain, GA, June 1–5, 1998, p. 541.
[10] M.W. Mahoney, C.G. Rhodes, J.G. Flintoff, R.A. Spurling, W.H. Bingel, Metall. Mater. Trans. A 29 (1998) 1955.
[11] Y.S. Sato, H. Kokawa, M. Enomoto, Metall. Mater. Trans. A 30 (1999) 2429.
[12] S. Benavides, Y. Li, L.E. Murr, D. Brown, J.C. McClure, Scripta Mater. 41 (1999) 809.
[13] L. Liu, H. Nakayama, S.J. Fukumoto, A. Yamamoto, H. Tsubakino, Mater. Trans. 45 (2004) 288.
[14] S. Lim, S. Kim, C.G. Lee, S. Kim, Metall. Mater. Trans. A 35 (2004) 2837.
[15] B.J. Dracup, W.J. Arbegast, in: Proceedings of the 1999 SAE Aerospace Automated Fastening Conference and Exposition, Memphis, TN, October 5–7, 1999.
[16] A. von Strombeck, J.F. dos Santos, F. Torster, P. Laureano, M. Koçak, in: Proceedings of the First International Symposium on Friction Stir Welding, Thousand Oaks, CA, June 14–16, 1999.